PCCP
Physical Chemistry Chemical Physics

Accepted Manuscript

This article can be cited before page numbers have been issued, to do this please use: G. Saielli, *Phys. Chem. Chem. Phys.*, 2026, DOI: 10.1039/D6CP01530A.

ROYAL SOCIETY OF CHEMISTRY

rsc.li/pccp

View Article Online
DOI: 10.1039/D6CP01530A

Relativistic DFT-NMR of ^{19}F in Tantalum(V) and Niobium(V) Fluorohalides

Giacomo Saielli[a,b*]

[a]CNR – ITM, Institute on Membrane Technology "Enrico Drioli", Padova Unit, Via Marzolo, 1, 35131 Padova, Italy

[b]Department of Chemical Sciences, University of Padova, Via Marzolo 1, 35131 Padova, Italy

Corresponding Author

*giacomo.saielli@unipd.it.

KEYWORDS: Relativistic DFT, Fluorine, Computational NMR, Tantalum, Niobium

ABSTRACT

The ^{19}F NMR chemical shift in tantalum(V) and niobium(V) fluorohalides of general formula $MF_nX_mY_l^-$ (M = Ta, Nb; X, Y = Cl, Br; $n+m+l=6$, $n \geq 1$) is investigated by means of relativistic DFT calculations. A systematic benchmark of 21 computational protocols is presented, varying the density functional (BLYP, B3LYP, BH&HLYP, PBE0), the basis set (DZ to QZ4P), the

View Article Online
DOI: 10.1039/D6CP01530A

geometry optimization scheme, the inclusion of solvent effects via PCM or COSMO continuum models, and the type of Hamiltonian: non-relativistic, two-component ZORA scalar, two-component ZORA spin-orbit, and relativistic 4-component. The spin-orbit contribution to the fluorine shielding constant is found to be substantial, ranging from approximately 8 to 19 ppm across the series, confirming the importance of properly accounting for relativistic effects in these heavy-metal systems. The best agreement with experimental data is achieved at the ZSO-B3LYP(COSMO)/QZ4P level of theory, using geometries optimized at the ω-B97XD(PCM)/def2-TZVPP level, with correlation coefficients close to unity and mean absolute errors below 5 ppm for the tantalum series. Calculated chemical shifts are also reported for all 46 possible fluorohalide structures (containing at least one fluorine atom) of tantalum(V) and niobium(V), including those not experimentally detected. Finally, a re-examination of the experimental ^{19}F NMR data reveals a likely misassignment in the niobium(V) series: the resonance originally attributed to the fluorine atom trans to bromine in cis-$NbF_4Br_2^-$ deviates by more than 50 ppm from the computed value and from the expected linear correlation between isostructural Ta(V) and Nb(V) complexes, suggesting an incorrect structural assignment in the original work.

INTRODUCTION

Fluorine NMR is a very powerful technique to investigate the structure of fluorinated chemical systems, including biologically relevant compounds through chemical labelling,[1,2] since ^{19}F has a natural abundance of 100% and a spin ½, making it an ideal probe for NMR.[3] In parallel with the

View Article Online
DOI: 10.1039/D6CP01530A

experimental developments of ^{19}F NMR, a significant effort has been devoted to the prediction, by quantum chemical methods, mostly based on DFT, of the fluorine shielding constant.[4–13] Fedorov and Krivdin[4] systematically investigated computational schemes for ^{19}F NMR chemical shifts, focusing on the development of "locally dense basis sets" to balance accuracy and computational cost. The computational protocols were then applied to fluorobenzenes in a subsequent study.[5] Rusakova et al. systematically evaluated DFT functionals and basis sets for computing ^{19}F NMR chemical shifts, ultimately recommending the pcS-3/pcS-2 locally dense basis set scheme as the most balanced approach for fluorine shift calculations in organic molecules[10] and in the presence of iodine atoms.[11] Moreover, the importance of basis-set artificially saturated in the tight *s*-region was discussed.[14] A computational protocol specifically targeting ^{19}F in PFAS (per- and polyfluoroalkyl substances) was developed by Mifkovic et al.[15] We also contributed to the field by investigating the relativistic effects in various fluorides, including uranium derivatives[16,17] and organic fluorinated compounds.[18] Relatively low-level DFT methods, using a scaling factor for predicting ^{19}F NMR shifts in fluorinated (hetero)aromatic compounds were introduced in Ref. [7] while inexpensive DFT protocols were tested in Ref.[8]. A recent thorough benchmark study was also reported in Ref. [9], concerning fluorinated organic molecules. Computational tools for compounds containing fluorine-carbon and fluorine-boron bonds were reported by Dumon et al. [12] while in a recent paper Krampe et al. investigated fluorine chemical shifts in iron complexes.[13] Finally, a recent paper by Gonnella and co-workers[19] found that B3LYP is providing a very good performance for the prediction of ^{19}F NMR in organic molecules.

When heavy atoms are present, relativistic versions of DFT need to be used to recover the scalar and most notably the spin-orbit effect.[20–22] The relativistic effects are one of the three main sources of structural complexity that can hamper the interpretation of the NMR spectra, the other two being

View Article Online
DOI: 10.1039/D6CP01530A

the topological complexity of the molecule, e.g. natural products, and systems with strong solute-solvent interactions. These issues, and what type of protocol should be used to overcome such difficulties, have been investigated in detail in a recent Account. [23]

In the literature, relativistic effects on the NMR properties have been classified into three main types: HALA (Heavy Atom on Light Atom) effect, when the presence of a heavy atom influences the chemical shift of light atoms, such as ^{1}H and ^{13}C, bonded to it; the effect is primarily due to the spin-orbit (SO) coupling in the Hamiltonian. It was originally noted by Nomura et al.,[24] and further theoretically developed by several other groups.[25–28] On the other hand, the HAHA effect (Heavy Atom on the Heavy Atom) refers the relativistic effects of the heavy atoms on its own NMR properties, which also depend on SO coupling and other contributions.[29–32] Finally, the HAVHA effect (Heavy Atom on Vicinal Heavy Atom) is referred to the case where a heavy atom is affecting the chemical shift of another heavy atom, chemically bonded to the first one.[33–36] A comprehensive review on heavy atom effects on NMR chemical shifts can be found in Ref. [37].

Tantalum and Niobium are transition metals that could be investigated directly by NMR, having NMR active isotopes. Nonetheless, the large majority of papers found in the literature concerning NMR of Ta and Nb compounds deal with the NMR of the ligands, as noted in the comprehensive review paper by Xue and Cook.[38] An example of such investigations, dating back to 1974, is the report by Buslaev and Ilyin.[39] The Authors measured, with respect to the resonance of F_2, the ^{19}F chemical shift of several tantalum(V) and niobium(V) fluorohalides, $MF_nX_mY_l^-$, with (M = Ta, Nb; X, Y = Cl, Br; $n + m + l = 6$; $n \overset{24}{12} 1$). In particular, they prepared fluorochlorides and fluorobromides of tantalum by mixing either $TaCl_5$ or $TaBr_5$ with HF in acetonitrile, as well as chloro/bromo mixed fluorides by mixing the original solutions and allowing the system to reach equilibrium. In contrast, for the niobium derivatives, only the fluorochlorides and fluorobromides were prepared

View Article Online
DOI: 10.1039/D6CP01530A

by mixing $NbCl_5$ or $NbBr_5$ with HF in acetonitrile. The experimental chemical shift data span a range of about 170 ppm, from 222 ppm of *trans*-$NbF_2Br_4^-$ to 389 ppm of TaF_6^-. This is a rather large range considering that in all cases fluorine is bonded to either Ta or Nb. Although the two metal ions are chemically quite similar, due to the lanthanide contraction, the two ranges are only partly overlapped: the range of experimental ^{19}F chemical shifts, with respect to F_2, is approximately from 290 to 390 ppm for the tantalum derivatives, while it is approximately from 220 to 330 for the niobium derivatives. Clearly, relativistic effects are expected to play a role, especially for the tantalum derivatives. It is, therefore, the aim of this work, to systematically investigate the performance of several DFT based protocols for the prediction of the ^{19}F chemical shift in these compounds. We will test different functionals and basis sets, the effect of the solvent reaction field and the type of model Hamiltonian: non-relativistic, ZORA scalar and ZORA spin orbit as well as relativistic 4-component.

In addition to the calculation of $\delta(^{19}F)$ for the compounds studied in Ref. [39], we also report here the analogous data for the other fluorohalides of tantalum and niobium not experimentally observed by Buslaev and Ilyin. One of the interesting results of our investigation is the identification of a misassigned resonance for a niobium(V) fluorobromide: some possible structural reassignments will be discussed.

COMPUTATIONAL SECTION

Geometry optimizations were run with the software Gaussian 16[40] and ADF 2019.[41,42] All structures were checked, at all levels of theory used for the optimizations, to be true minima by verifying the absence of imaginary frequencies at the stationary point. The ^{19}F NMR shielding

View Article Online
DOI: 10.1039/D6CP01530A

constant, σ, at the non-relativistic (NR), two-component ZORA Scalar Relativistic (ZSC) and two-component ZORA Spin-orbit Relativistic (ZSO) levels[43,44] were calculated with the software ADF, while 4-component relativistic calculations were run with the software ReSpect.[45,46] Since all experimental data were measured in acetonitrile,[39] when the solvent reaction field was used in the calculation we used the PCM model,[47,48] with the default implementation in Gaussian 16, or the COSMO model,[49] with the default implementation in ADF, respectively, with a dielectric constant $\varepsilon_0 = 35.688$.

Geometry Optimizations. Different levels of theory were tested concerning the geometry optimization. With ADF these are ZSC-BP(COSMO)/TZ2P,[50,51] ZSC-B3LYP/TZ2P,[52] ZSC-B3LYPG3/TZ2P which includes the dispersive interactions Grimme3 BJDAMP,[53] ZSC-B3LYPG3(COSMO)/TZ2P and ZSC-PBE0G3(COSMO)/TZ2P.[54] With Gaussian 16 we run optimization at the ω-B97XD/def2-TZVPP level[55–57] and the analogous ω-B97XD(PCM)/def2-TZVPP including the solvent reaction field. In this cases the def2-TZVPP basis set were downloaded from the Basis Set Exchange web site.[58–60]

NMR calculations. Fluorine shielding constants, σ, were calculated at several levels of theory, either using ADF or Respect and the functional BLYP,[50,61] PBE0,[54] BH&HLYP,[62] B3LYP.[52] These levels are listed in Table 1.

Table 1. Levels of theory used in this work for Ta(V) and Nb(V) fluorohalides. The column "Note" suggests the other level with the smallest difference in the computational protocol for a direct comparison. Lowercase roman numerals are used in the rest of the manuscript for quicker reference to the specific level of theory.

View Article Online
DOI: 10.1039/D6CP01530A

OPT level	NMR level	Note	Level
ZSC-BP(COSMO)/ TZ2P	ZSO-PBE0/DZ	GGA functional in OPT step, lowest basis set in NMR step	**i**)
	ZSO-PBE0/TZP	Larger basis set w.r.t. **i**)	**ii**)
	ZSO-PBE0/TZ2P	Larger basis set w.r.t. **ii**)	**iii**)
	ZSO-PBE0/QZ4P	Larger basis set w.r.t. **iii**)	**iv**)
	ZSO-PBE0(COSMO)/QZ4P	Solvent effect w.r.t. **iv**)	**v**)
	ZSC-PBE0(COSMO)/QZ4P	Scalar ZORA w.r.t. **v**)	**vi**)
ZSC-B3LYP/ TZ2P	ZSO-PBE0(COSMO)/QZ4P	Hybrid functional in OPT step w.r.t. **v**)	**vii**)
ZSC-B3LYPG3/ TZ2P	ZSO-PBE0(COSMO)/QZ4P	Dispersive correction in OPT step w.r.t. **vii**)	**viii**)
ZSC-B3LYPG3 (COSMO)/ TZ2P	ZSO-PBE0(COSMO)/QZ4P	Solvent effect in OPT step w.r.t. **viii**)	**ix**)
	ZSO-BH&HLYP (COSMO)/QZ4P	Different functional in NMR step w.r.t. **ix**)	**x**)
ZSC-PBE0G3 (COSMO)/ TZ2P	ZSO-PBE0(COSMO)/QZ4P	Different functional in OPT step w.r.t. **ix**)	**xi**)
ω-B97XD(PCM)/ def2-TZVPP	ZSO-BH&HLYP (COSMO)/QZ4P	Different functional in OPT step w.r.t. **x**)	**xii**)
	ZSC-BH&HLYP (COSMO)/QZ4P	Scalar ZORA w.r.t. **xii**)	**xiii**)
	ZSO-B3LYP (COSMO)/QZ4P	Different functional w.r.t. **xii**)	**xiv**)

View Article Online
DOI: 10.1039/D6CP01530A

	ZSO-PBE0 (COSMO)/QZ4P	Different functional w.r.t. **xii**) and **xiv**)	**xv**)
	ZSO-BLYP (COSMO)/QZ4P	Different functional w.r.t. **xii**), **xiv**) and **xv**)	**xvi**)
	ZSO-B3LYP/QZ4P	No solvent in NMR step w.r.t. **xiv**)	**xvii**)
	mDKS-B3LYP/vqz	4-component Hamiltonian w.r.t. **xiv**)	**xviii**)
	ZSO-B3LYP (COSMO)/TZ2P	Smaller basis set w.r.t. **xiv**)	**xix**)
	ZSO-B3LYP (COSMO)/TZP	Smaller basis set w.r.t. **xix**)	**xx**)
ω-B97XD/ def2-TZVPP	ZSO-B3LYP (COSMO)/QZ4P	No solvent in OPT step w.r.t. **xiv**)	**xxi**)

Experimental values are reported in Ref. [39] with respect to F_2 and with the convention of an opposite sign compared to the modern definition. Therefore, in order to compare calculated and experimental chemical shifts, we define here the calculated fluorine chemical shift, δ, as

$$\delta = \frac{\sigma - \sigma_{ref}}{1 - \sigma_{ref}} + \delta_{F_2} \approx \sigma - \sigma_{ref} + \delta_{F_2} \qquad 1)$$

where σ is the calculated shielding constant of ^{19}F in the compound of interest, σ_{ref} is the shielding constant of ^{19}F in the standard reference, $CFCl_3$, calculated at the same level of theory, while δ_{F_2} is the experimental chemical shift of F_2 with respect to the standard reference, $CFCl_3$, used to scale the calculated results and amounting to +422.92 ppm.[63] It is worth mentioning that the

View Article Online
DOI: 10.1039/D6CP01530A

approximation involved in the second equality in Eq. 1) holds since the shielding constants are expressed in part-per-million, therefore even in cases of shielding constants of the order of 10^3, σ_{ref} in the denominator can be safely neglected with respect to 1.

RESULTS AND DISCUSSION

There are 46 possible combinations of F, Cl and Br to form octahedral complexes with at least one F atom, and they are shown in Figure 1.

View Article Online
DOI: 10.1039/D6CP01530A

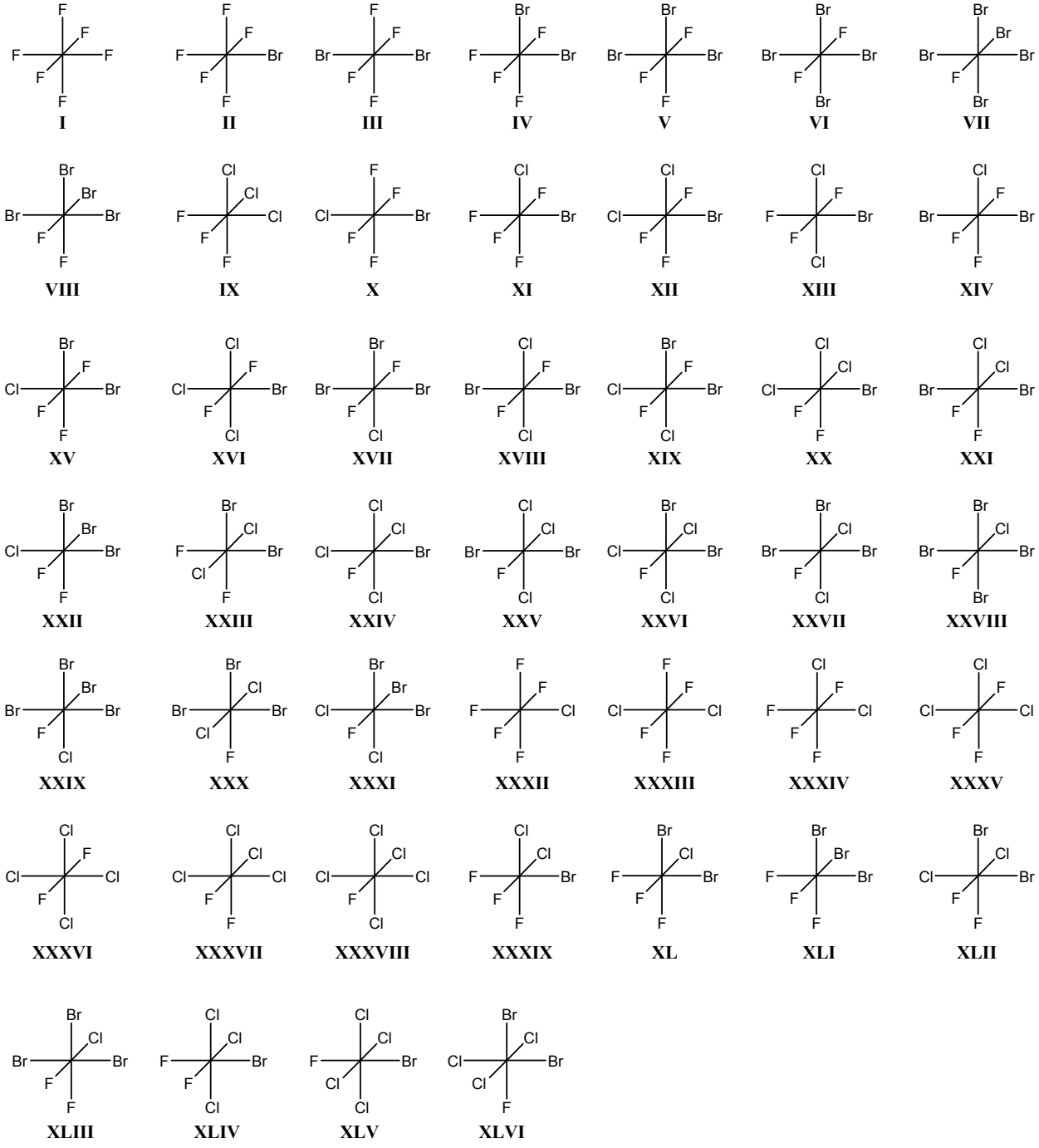

Figure 1. Tantalum(V) and niobium(V) fluorohalides studied in this work of general formula $MF_nX_mY_l^-$ (M = Ta, Nb; X, Y = Cl, Br; $n + m + l = 6$, $n \overset{24}{12} 1$). The metal (either Ta or Nb) at the center of the octahedron is removed for clarity. All complexes are anionic with a charge of -1.

View Article Online
DOI: 10.1039/D6CP01530A

The complexes are numbered using uppercase roman numerals, following the original publication, where possible:[39] from **I** to **XXXVIII** they have been experimentally observed, while complexes from **XXXIX** to **XLVI** (having no fluorine atoms in trans to each other) were not detected by NMR. In addition, we should note that for compounds **XIII**, **XIV** and **XV**, exhibiting two types of fluorine atoms, Buslaev and Ilyin only reported the resonance of fluorine atoms in trans to each other (labeled as F1 type), while the experimental value of the other F atom (in trans to Br in **XIII** and **XV** and in trans to Cl in **XIV** and labeled as F2 type) was not observed.

All correlation graphs of calculated vs experimental $\delta(^{19}F)$ are reported in Electronic Supporting Information (ESI), Figures S1-S21. Here we will limit our discussion to the statistical parameters used to gauge the performance of a given level of theory, see Figure 2 (and Table S1 in ESI). These parameters are: the correlation coefficient of the linear fitting, R^2; the slope, a, and the intercept, b, of the linear fitting,

$$\delta(^{19}F)_{calc} = a\,\delta(^{19}F)_{expt} + b \qquad 2)$$

(the parameters b are only in Table S1 of ESI); the mean absolute error, MAE, defined as

$$MAE = (\Sigma_n|\delta(^{19}F)_{calc} - \delta(^{19}F)_{expt}|)/N, \qquad 3)$$

where N is the number of datapoints in the correlation and n runs over them; the maximum error, MaxErr, that is the maximum difference of the set of absolute values of calculated and experimental chemical shifts:

$$MaxErr = MAX(\ |\delta(^{19}F)_{calc} - \delta(^{19}F)_{expt}|\ ). \qquad 4)$$

View Article Online
DOI: 10.1039/D6CP01530A

We begin our discussion with a test of the basis set effect in the NMR calculation using the ZSO Hamiltonian and PBE0 functional. Comparison of the statistical parameters for levels **i**)-**iv**) suggests that a systematic improvement is obtained increasing the size of the basis set up to QZ4P (the largest available in ADF). The correlation coefficient increases, and the MAE and MaxErr decrease with the basis set size; the improvement using the QZ4P basis set is not negligible, therefore it will be used throughout the rest of the paper. The slope and the intercept of the linear fitting have a somewhat less clear trend, in particular the small DZ basis set provides values close to 1 and 0, respectively, but with clearly a much worse overall correlation (see Figure S1 in ESI).

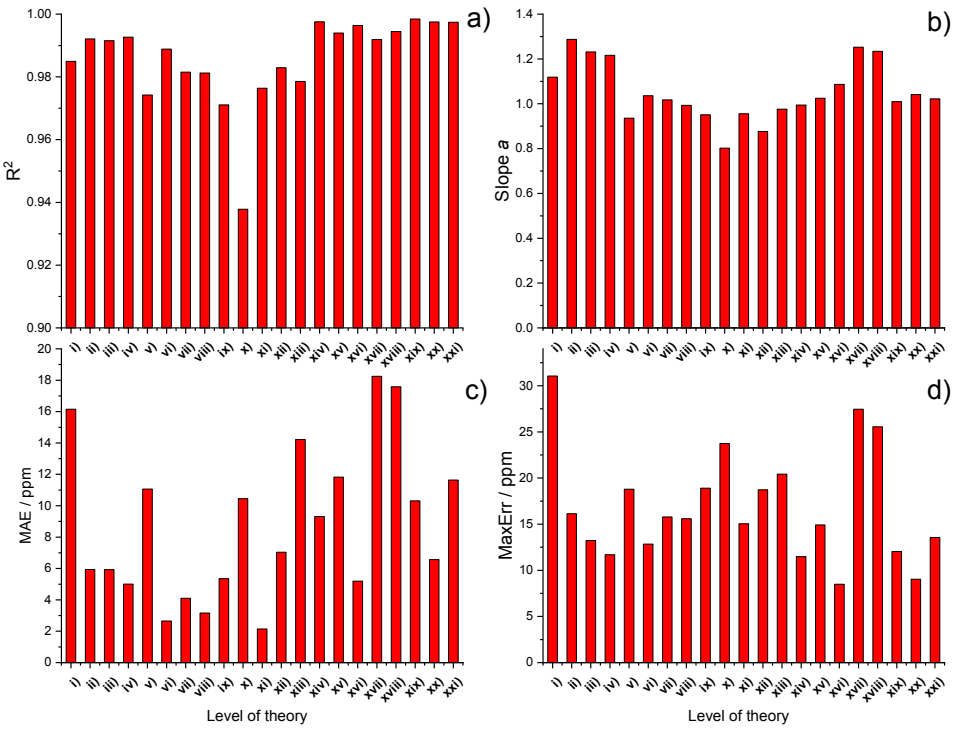

Figure 2. Statistical parameters for the various levels of theory used. a) Correlation coefficient, R^2; b) slope of the linear fitting line, *a*; c) Mean Absolute Error, MAE, in ppm; d) Maximum Error, MaxErr, in ppm.

View Article Online
DOI: 10.1039/D6CP01530A

Inclusion of the solvent reaction field in the NMR calculation seems to worsen the agreement, using these geometries, see level **v**). To test the importance of the SO coupling, we have calculated the chemical shifts also at the ZSC method, see level **vi**). The SO contribution, σ_{SO}, obtained simply as the difference between the shielding constants calculated at the ZSO, level **v**) and ZSC, level **vi**), is significant for an accurate prediction: it varies from a minimum of 7.62 ppm (positive values indicates a shielding contribution) for TaF_6^- (**I**) to a maximum of 18.74 ppm and 18.89 ppm for $TaFBr_5^-$ (**VII**) and *trans*-$TaFClBr_4^-$ (**XXVIII**), respectively. Although the well-known HALA and HAVHA effects mentioned in the Introduction refer to atoms directly bonded to the nucleus of interest, it appears that the SO shielding effect on the chemical shift can be transmitted to nuclei separated by more than one bond. The overall agreement, however, is not particularly good using these geometries.

We then tested the effect of using different optimization schemes. Levels **vii**)-**ix)** and **xi**) refers to NMR calculations at the ZSO-PBE0(COSMO)/QZ4P for geometries optimized with various "improvements" in the level of theory of the optimization step: hybrid functional B3LYP instead of the GGA BLYP, addition of the dispersive correction, addition of long-range solvent effects, a different hybrid functional (PBE0). For the last optimization protocol, we have also calculated the chemical shift with the BH&HLYP functional, level **x**). Surprisingly, the correlation gets worse as the optimization protocol is theoretically improved by including additional effects. Particularly poor is the correlation between calculated and experimental data using the BH&HLYP functional

View Article Online
DOI: 10.1039/D6CP01530A

for the NMR properties, level **x**), see Figure S10. Finally, we selected, as optimization method, the ω-B97XD(PCM)/def2-TZVPP using Gaussian 16. Here, relativistic effects are included only through effective core potentials, while the ω-B97XD functional includes both the long-range correction and the dispersive interactions. We note that the same optimization protocol was successfully used in previous works with heavy elements, such as organometallic compounds of thallium,[64] iridium,[65] and tetrahalogeno-indates and gallates,[66] as well as polyalogenated natural products,[67] generally resulting in a very good agreement between calculated and experimental geometries as well as the ensuing NMR properties. Using these geometries, we calculated the chemical shifts with several protocols, levels **xii**)-**xx**). The agreement appears to be significantly increased, the correlation coefficients are in most cases close to unity. The best performance is obtained using the B3LYP functional with either QZ4P, level **xiv**) or TZ2P basis set, level **xix**), and with the inclusion of the solvent reaction field also in the NMR calculation, see Figure S14. This result is in agreement with the observation of Gonnella[19] concerning the good performance of B3LYP to predict fluorine chemical shifts. Other protocols have lower MAE and/or MaxErr but a slightly worse linear correlation, therefore a lower predictive power. As an example, the correlation graph of calculated vs experimental δ(^{19}F) in tantalum fluorohalides for level of theory **xiv**) are shown in Figure 3. The main source of error appears to be a systematic shift of the calculated values, which, for practical applications, can also be empirically compensated.

View Article Online
DOI: 10.1039/D6CP01530A

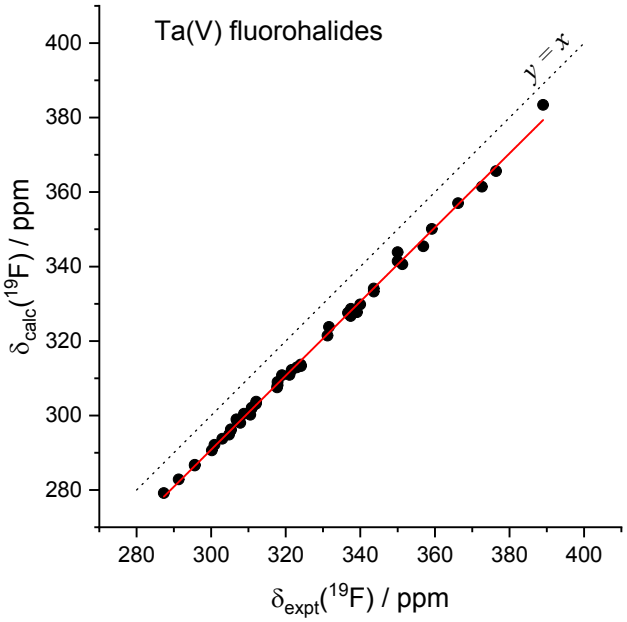

Figure 3. Correlation between calculated and experimental fluorine chemical shifts (w.r.t. F_2) at level of theory **xiv**) for the tantalum(V) fluorohalides investigated in Ref. [39]. The red line is the linear fit, the dotted black line the ideal correlation $y = x$. Fitting parameters can be found in ESI, Figure S14.

It is worth mentioning that the conclusion about the best performance is mostly based on the value of the R^2 parameter. In fact, as can be seen in Figure 2 and Figure S11 of ESI, the level of theory **xi**) also appears very good with a rather low MAE, suggesting that the absolute value of the chemical shift is on average much closer to the experimental values than in the other cases. However, two points are worth noting: first, the experimental values are measured, as stated in the original paper,[39] with respect to F_2, but the exact experimental procedure is not detailed. For example, pressure effects in the NMR tube might introduce a systematic constant additional term

View Article Online
DOI: 10.1039/D6CP01530A

which would shift the correlation graph along the *y* axis, therefore altering the MAE, but not R^2 values. Secondly, the predictive power of a computational protocol is related with its ability to put all the calculated values perfectly – or as much as possible – in order in a correlation graph. In this respect, a constant shift would not hamper the possibility to use the protocol to make valuable predictions. For these reasons, here we prefer to select the level of theory **xiv**), keeping in mind that level **xi**) is in fact closer to the absolute values.

In Table 2 we report the experimental chemical shifts of Ref. [39] together with the calculated shielding constants and calculated chemical shifts obtained at the level of theory **xiv**) using Eq. 1).

Table 2. Experimental chemical shifts and calculated shielding constants and chemical shifts (w.r.t. F_2) at level **xiv**) for the tantalum(V) fluorohalides of Figure 1.

Mol	F type[a]	$\delta_{expt}(^{19}F)$ / ppm[b]	$\sigma_{calc}(^{19}F)$ / ppm	$\delta_{calc}(^{19}F)$ / ppm
$CFCl_3$		422.9	175.4	422.9
I	F1	389.0	135.9	383.4
II	F1	359.2	102.6	350.1
II	F2	372.6	113.9	361.5
III	F1	331.6	76.3	323.8
IV	F1	331.2	73.9	321.4
IV	F2	351.3	93.1	340.6
V	F1	307.0	51.1	298.6
V	F2	336.7	80.1	327.6

View Article Online
DOI: 10.1039/D6CP01530A

VI	F1	287.3	31.6	279.2
VII	F2	306.8	51.5	299.0
VIII	F2	319.0	63.3	310.8
IX	F2	339.1	80.2	327.7
X	F1	337.5	81.1	328.6
XI	F1	337.0	79.7	327.2
XI	F2 Br	350.0	96.3	343.9
XI	F2 Cl	350.0	93.9	341.4
XII	F1	317.8	60.6	308.1
XII	F2	337.4	79.2	326.7
XIII	F1	317.7	60.0	307.5
XIII	F2	-	83.5	331.0
XIV	F1	312.1	56.2	303.7
XIV	F2	-	77.4	324.9
XV	F1	312.0	55.6	303.1
XV	F2	-	82.0	329.6
XVI	F1	300.2	43.1	290.6
XVII	F1	291.3	35.3	282.8
XVIII	F1	295.6	39.1	286.6
XIX	F1	295.6	39.2	286.7
XX	F2	321.0	63.4	310.9
XXI	F2	317.8	61.5	309.0

View Article Online
DOI: 10.1039/D6CP01530A

XXII	F2	321.6	64.7	312.3
XXIII	F2	324.0	66.2	313.7
XXIV	F2	307.8	50.5	298.0
XXV	F2	305.3	48.8	296.3
XXVI	F2	305.3	48.5	296.0
XXVII	F2	303.0	46.2	293.8
XXVIII	F2	300.9	44.6	292.1
XXIX	F2	308.8	53.0	300.5
XXX	F2	310.9	54.6	302.1
XXXI	F2	310.9	54.5	302.0
XXXII	F1	366.2	109.5	357.0
XXXII	F2	376.4	118.1	365.6
XXXIII	F1	343.6	86.6	334.1
XXXIV	F1	343.6	85.8	333.3
XXXIV	F2	356.9	97.9	345.4
XXXV	F1	323.0	65.4	312.9
XXXV	F2	340.0	82.3	329.8
XXXVI	F1	304.8	47.3	294.8
XXXVII	F2	324.1	65.8	313.3
XXXVIII	F2	310.5	52.7	300.2
XXXIX	F2 Br	-	80.3	327.8
XXXIX	F2 Cl	-	76.6	324.1

View Article Online
DOI: 10.1039/D6CP01530A

XL	F2 Br	-	78.0	325.5
XL	F2 Cl	-	72.7	320.2
XLI	F2	-	75.1	322.6
XLII	F2 Br	-	67.6	315.1
XLII	F2 Cl	-	60.7	308.2
XLIII	F2 Br	-	65.9	313.4
XLIII	F2 Cl	-	58.4	305.9
XLIV	F2 Br	-	69.0	316.5
XLIV	F2 Cl	-	62.8	310.3
XLV	F2	-	57.6	305.1
XLVI	F2	-	56.4	303.9

[a]F1 trans to F; F2 trans to halogen. [b]From Ref. [39], w.r.t. F_2.

Therefore, we selected the level **xiv**) for analogous calculations of the chemical shift of fluorine in some niobium fluorohalides also experimentally investigated in Ref. [39]. The result of the correlation between these calculated and experimental $\delta(^{19}F)$ is shown in Figure 4. It appears that one data point is largely off the expected result. It corresponds to the fluorine trans to Br (F2 type) in *cis*-$NbF_4Br_2^-$ (**IV**). The calculated chemical shift, 286.3 ppm, is more than 50 ppm larger than the experimental value, 230 ppm, reported in Ref. [39]. Such a large discrepancy is clearly outside the range of confidence of the linear correlation of Figure 4. Therefore, we can conclude that the assignment of Ref. [39] is not correct. This conclusion is also supported by a purely empirical consideration: in Figure 5 we show the fluorine resonance for isostructural Ta(V) and Nb(V)

View Article Online
DOI: 10.1039/D6CP01530A

fluorohalides and, again, the resonance of 230 ppm assigned to *cis*-$NbF_4Br_2^-$ (**IV**) clearly appears incorrect.

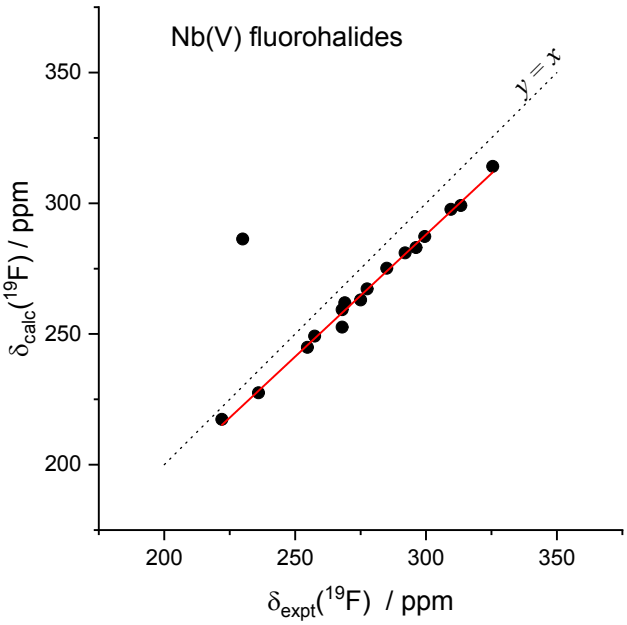

Figure 4. Correlation between calculated and experimental fluorine chemical shifts (w.r.t. F_2) at level of theory **xiv**) for the niobium(V) fluorohalides investigated in Ref. [39]. The red line is the linear fit excluding the outstanding datapoint (**IV**), the dotted black line is the ideal correlation $y = x$. Fitting parameters are in ESI, Figure S22.

View Article Online
DOI: 10.1039/D6CP01530A

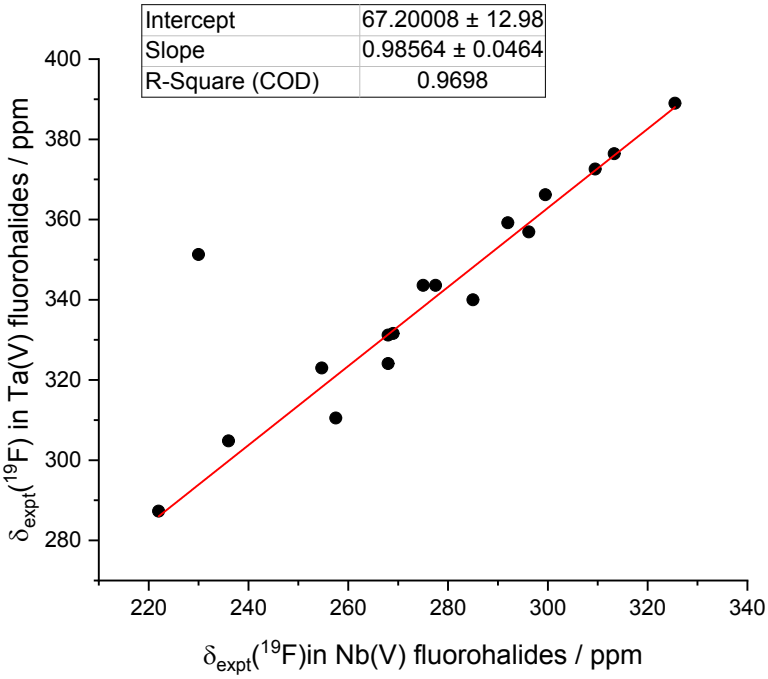

Figure 5. Correlation between experimental fluorine chemical shifts (w.r.t. F_2) of the niobium(V) and tantalum(V) isostructural fluorohalides investigated in Ref. [39]. The red line is the linear fit excluding the outstanding datapoint originally assigned to complex (**IV**).

Interestingly, the results shown in Figure 5 seem to suggest that the fluorine chemical shift, as the metal center changes from Nb to Ta, just changes by a constant additional shielding contribution of approximately 67 ppm (we should recall here the opposite sign convention of Ref. [39]). This contribution is partly related to the HALA effect of the heavier tantalum atom compared with niobium on the fluorine chemical shift. However, other electronic effects are clearly in place, as noted already by Buslaev and Ilyin, who attributed the systematic shift to a more covalent character

View Article Online
DOI: 10.1039/D6CP01530A

of the Nb-F bond compared to the Ta-F bond in isostructural complexes.[39] This empirical observation was based on larger values of $^{2}J(^{19}F,^{19}F)$ in niobium fluorochloro complexes (54 Hz) compared to that one in the homologous tantalum fluorochloro complexes (36 Hz).[39] In fact, if we compare the SO correction to the shielding constant for the homologous compounds reported in Figure 5 (see Table S2 in ESI) we note that, although this is generally larger in the tantalum derivatives with respect to the niobium derivatives, it does not account for the full shift when replacing niobium with the heavier tantalum in a given complex. This is confirmed by inspection of Figure 6, where we show the analogous dependence shown in Figure 5 above, but now using the calculated shielding constants of all Ta(V) and Nb(V) compounds of Figure 1, rather than the few experimental chemical shifts available for both metals. Since the shielding constants and the chemical shifts are related simply by Eq. 1), we expect the same fitting line of Figure 5 to "pass through" the calculated points of Figure 6 as well. Indeed, several data points lie close to the line, however, many others now form clusters of points quite far from the expected linear prediction. This indicates that other electronic effects, likely related with the position of the fluorine atom in the cluster (*cis* or *trans* to another F, Cl, or Br), the extent of back donation form the Cl and Br ligands into the metal orbitals, as well as paramagnetic effects related with the Cl and Br lone pairs, have a major influence on the ^{19}F chemical shift, besides the HALA contribution of the metal center.

View Article Online
DOI: 10.1039/D6CP01530A

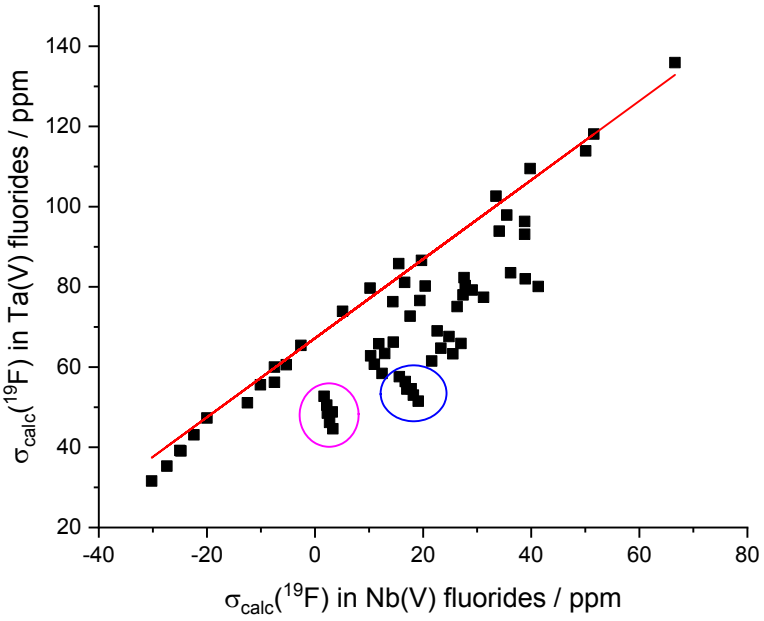

Figure 6. Correlation between calculated fluorine shielding constants of the niobium(V) and tantalum(V) isostructural fluorohalides. The red line is the same linear fitting line as in Figure 5. Data points in the blue and magenta circles are discussed in the main text.

As an example, the data in the blue circle in Figure 6 represent the results of complexes **VII**, **XXIX**, **XXX**, **XLVI** and **XLV** (plus the structural isomer **XXXI**) where a single fluorine is in trans to Br and the other four Br atoms in the perpendicular plane of the octahedral structure of **VII** ($MFBr_5^-$) are successively replaced by 1, 2, 3 and 4 Cl atoms, respectively. Similarly, the data in the magenta circle represent the analogous series where Cl and Br have reversed their role (and positions), that is complexes **XXXVIII** ($MFCl_5^-$), **XXIV** (plus the structural isomer **XXV**), **XXVI**, **XXVII** and **XXVIII**. The trends in these subsets, although apparently simple, likely depend on a very subtle balance of several electronic effects since they show an opposite direction for Ta and Nb: as the

View Article Online
DOI: 10.1039/D6CP01530A

Cl atoms replace the equatorial Br atoms in $MFClBr_4^-$ (**XXVIII**) and $MFBr_5^-$ (**VII**), the ^{19}F resonance is increasingly shielded in the niobium complexes and increasingly de-shielded in the tantalum complexes.

Having now calculated also the fluorine chemical shift for all the remaining niobium compounds of Figure 1, we can search for the complexes which are in agreement with the erroneously assigned resonance discussed above. The results are shown in Table 3. It appears that few compounds exhibit a fluorine chemical shift which is perfectly within the expected correlation, these are *trans*-NbF_2Cl_3Br (**XVI**), *trans*-NbF_2ClBr_3 (**XVII**), *trans*-$NbF_2Cl_2Br_2$ (**XVIII**) and *trans*-$NbF_2Cl_2Br_2$ (**XIX**). In all cases, the fluorine atoms are in trans to each other. Based on the calculated values, all very close, it is not possible to single out one of the four complexes as the correct compounds originating the observed resonance. It is also important to stress that all these complexes, containing both chloride and bromide, should not be present in the original solutions, based on the reported experimental procedure for the preparation.

Table 3. Experimental chemical shifts and calculated shielding constants and chemical shifts (w.r.t. F_2) at level **xiv**) for the niobium(V) fluorohalides of Figure 1.

Mol	F type[a]	$\delta_{expt}(^{19}F)$ / ppm[b]	$\sigma_{calc}(^{19}F)$ / ppm	$\delta_{calc}(^{19}F)$ / ppm
I	F1	325.5	66.6	314.1
II	F1	292.0	33.5	281.0

View Article Online
DOI: 10.1039/D6CP01530A

II	F2	309.5	50.1	297.7
III	F1	269.0	14.4	261.9
IV	F1	268.0	5.1	252.6
IV	F2	230.0	38.8	286.3
V	F1		-12.5	235.0
V	F2		41.3	288.8
VI	F1	222.0	-30.2	217.4
VII	F2		19.1	266.6
VIII	F2		25.5	273.0
IX	F2		20.4	267.9
X	F1		16.6	264.1
XI	F1		10.2	257.7
XI	F2 Br		38.8	286.3
XI	F2 Cl		34.1	281.7
XII	F1		-5.3	242.3
XII	F2		29.1	276.6
XIII	F1		-7.5	240.0
XIII	F2		36.2	283.7
XIV	F1		-7.5	240.0
XIV	F2		31.2	278.7
XV	F1		-10.1	237.4
XV	F2		38.9	286.4

View Article Online
DOI: 10.1039/D6CP01530A

XVI	F1		-22.4	225.2
XVII	F1		-27.4	220.1
XVIII	F1		-24.8	222.8
XIX	F1		-25.0	222.5
XX	F2		12.9	260.4
XXI	F2		21.6	269.1
XXII	F2		23.3	270.8
XXIII	F2		14.5	262.0
XXIV	F2		2.2	249.7
XXV	F2		3.2	250.7
XXVI	F2		2.3	249.9
XXVII	F2		2.7	250.2
XXVIII	F2		3.3	250.8
XXIX	F2		18.2	265.7
XXX	F2		17.8	265.3
XXXI	F2		17.0	264.5
XXXII	F1	299.5	39.8	287.3
XXXII	F2	313.3	51.6	299.1
XXXIII	F1	277.5	19.7	267.2
XXXIV	F1	275.0	15.5	263.0
XXXIV	F2	296.2	35.5	283.0
XXXV	F1	254.7	-2.6	244.9

View Article Online
DOI: 10.1039/D6CP01530A

XXXV	F2	285.0	27.6	275.2
XXXVI	F1	236.0	-20.0	227.5
XXXVII	F2	268.0	11.8	259.3
XXXVIII	F2	257.5	1.7	249.2
XXXIX	F2 Br		27.8	275.3
XXXIX	F2 Cl		19.4	266.9
XL	F2 Br		27.4	274.9
XL	F2 Cl		17.6	265.1
XLI	F2		26.3	273.8
XLII	F2 Br		24.8	272.3
XLII	F2 Cl		11.0	258.5
XLIII	F2 Br		27.0	274.5
XLIII	F2 Cl		12.4	259.9
XLIV	F2 Br		22.6	270.2
XLIV	F2 Cl		10.3	257.8
XLV	F2		15.6	263.1
XLVI	F2		16.7	264.2

[a]F1 trans to F; F2 trans to halogen. [b]From Ref. [39], w.r.t. F_2.

View Article Online
DOI: 10.1039/D6CP01530A

CONCLUSIONS

The prediction of ^{19}F NMR chemical shifts in tantalum(V) and niobium(V) fluorohalides was systematically investigated using a variety of relativistic DFT protocols, differing in functional, basis set, geometry optimization scheme, and model Hamiltonian. The following main conclusions can be drawn.

The spin-orbit (SO) contribution to the fluorine shielding constant is significant and cannot be neglected: it ranges from about 8 ppm in TaF_6^- (**I**) to nearly 19 ppm in $TaFBr_5^-$ (**VII**) and trans-$TaFClBr_4^-$, (**XXVIII**) confirming the importance of using a spin-orbit relativistic Hamiltonian (ZORA spin-orbit or 4-component) for an accurate description of the HALA and HAVHA effects in these heavy-metal systems.

The choice of geometry optimization protocol has a substantial impact on the quality of the NMR predictions. The best overall agreement with experiment is achieved when geometries are optimized at the ω-B97XD(PCM)/def2-TZVPP level, which incorporates long-range corrections, dispersion interactions, and solvent effects through effective core potentials. This result is in agreement with several previous reports.

Among the NMR protocols tested, ZSO-B3LYP(COSMO)/QZ4P - level **xiv**) - provides the best overall performance, in agreement with recent literature findings on the reliability of B3LYP for ^{19}F NMR predictions, at least based on the value of R^2 which measure the predictive power of a given protocol, that is the ability to predict even close resonances in the correct order. The QZ4P

View Article Online
DOI: 10.1039/D6CP01530A

basis set represents a systematic improvement over smaller basis sets, and its use is recommended. Inclusion of the solvent reaction field in the NMR step is beneficial when combined with the ω-B97XD geometries. It is, however, worth mentioning that other levels of theory provide a much better MAE, for example level **xi**) meaning chemical shift values on average closer to the experimental ones.

The experimental data for niobium(V) fluorohalides from Buslaev and Ilyin[39] were re-examined in light of the computed values. A clear outlier was identified in the correlation plot: the resonance assigned to the F2-type fluorine (trans to Br) in cis-$NbF_4Br_2^-$, compound (**IV**) shows a discrepancy of more than 50 ppm with respect to the calculated value, well outside the confidence range of the linear fit. This is further supported by the empirical linear correlation between ^{19}F chemical shifts in isostructural Ta(V) and Nb(V) complexes, which shows a nearly constant offset of approximately 67 ppm that can only in part be attributed to the HALA effect of the heavier tantalum. Moreover, when the comparison is extended to all complexes using the calculated shielding constant, several different trends appear, indicating a much more complex interplay of several electronic effects. The resonance at 230 ppm originally assigned to cis-$NbF_4Br_2^-$ (**IV**) appears to be misassigned; alternative structural candidates are trans-$NbF_3Cl_3Br^-$ (**XVI**), trans-$NbF_2ClBr_3^-$ (**XVII**), trans-$NbF_2Cl_2Br_2^-$ (**XVIII**), or trans-$NbF_2Cl_2Br_2^-$ (**XIX**), all of which yield calculated shifts consistent with the observed resonance. A definitive reassignment is not possible based solely on the computed data, due to the small differences in the resonances.

View Article Online
DOI: 10.1039/D6CP01530A

Calculated chemical shifts for the full set of 46 fluorohalide structures (including those not experimentally detected) are reported for both Ta(V) and Nb(V), providing a comprehensive computational reference for future experimental work.

ASSOCIATED CONTENT

AUTHOR INFORMATION

Corresponding Author

*Dr. G. Saielli

CNR – ITM Institute on Membrane Technology, Padova Unit, Via Marzolo, 1 – 35131, Padova, Italy.

E-mail: giacomo.saielli@unipd.it

Funding Sources

ACKNOWLEDGEMENT

CloudVeneto is acknowledged for the use of computing and storage facilities. We also thank the C3P community of the Department of Chemical Sciences for the allocation of computer time on several Linux clusters. This work was supported in part by the high-performance computing infrastructure developed under the project “CONVECS”, funded by the PR Veneto FESR 2021-2027 program, Priority 1 – Specific Objective 1.1 – Action 1.1.2.

View Article Online
DOI: 10.1039/D6CP01530A

REFERENCES

1 Y. Werle and M. Kovermann, *Chem. – A Eur. J.*, 2025, **31**, e202402820.

2 W. R. Dolbier, *Guide to Fluorine NMR for Organic Chemists*, 2008.

3 R. K. Harris, E. D. Becker, S. M. Cabral de Menezes, R. Goodfellow and P. Granger, *Solid State Nucl. Magn. Reson.*, 2002, **22**, 458–483.

4 S. V Fedorov and L. B. Krivdin, *J. Fluor. Chem.*, 2020, **238**, 109625.

5 S. A. Ukhanev, S. V Fedorov, Y. Y. Rusakov, I. L. Rusakova and L. B. Krivdin, *J. Fluor. Chem.*, 2023, **266**, 110093.

6 G. Saielli, A. Bagno, F. Castiglione, R. Simonutti, M. Mauri and A. Mele, *J. Phys. Chem. B*, 2014, **118**, 13963–13968.

7 C. Saunders, M. B. Khaled, J. D. Weaver and D. J. Tantillo, *J. Org. Chem.*, 2018, **83**, 3220–3225.

8 E. Benassi, *J. Comput. Chem.*, 2022, **43**, 170–183.

9 Y. Li, P. Zeng, Q. Lou, X. Su, W. Li and X. Wang, *J. Magn. Reson.*, 2024, **358**, 107611.

10 S. A. Ukhanev, Y. Y. Rusakov and I. L. Rusakova, *Int. J. Mol. Sci.*, 2025, 26, 6930.

11 I. L. Rusakova, S. A. Ukhanev and Y. Y. Rusakov, *J. Fluor. Chem.*, 2023, **271**, 110188.

View Article Online
DOI: 10.1039/D6CP01530A

12 A. S. Dumon, H. S. Rzepa, C. Alamillo-Ferrer, J. Bures, R. Procter, T. D. Sheppard and A. Whiting, *Phys. Chem. Chem. Phys.*, 2022, **24**, 20409–20425.

13 J. Krampe, T. Zankel, R. Kornievskii, K. Heckenberger, C. M. Thiele and V. Krewald, *Phys. Chem. Chem. Phys.*, , DOI:10.1039/D5CP04487A.

14 I. L. Rusakova and Y. Y. Rusakov, *Int. J. Mol. Sci.*, 2023, 24, 6231.

15 M. Mifkovic, J. Pauling and S. Vyas, *J. Comput. Chem.*, 2022, **43**, 1355–1361.

16 G. Saielli, R. Bini and A. Bagno, *Theor. Chem. Acc.*, , DOI:10.1007/s00214-012-1140-z.

17 G. Saielli, R. Bini and A. Bagno, *Theor. Chem. Acc.*, 2012, **131**, 1283.

18 G. Saielli, R. Bini and A. Bagno, *RSC Adv.*, 2014, **40**, 41605–41611.

19 R. K. Ghosh, G. A. Valdivia-Berroeta, D. Xin and N. C. Gonnella, *J. Org. Chem.*, 2025, **90**, 12050–12060.

20 Y. Xiao, W. Liu and J. Autschbach, ed. W. Liu, Springer Berlin Heidelberg, Berlin, Heidelberg, 2017, pp. 657–692.

21 J. Autschbach, *Philos. Trans. R. Soc. A Math. Phys. Eng. Sci.*, 2014, **372**, 20120489.

22 L. B. Krivdin, *Russ. Chem. Rev.*, 2021, **90**, 1166.

23 G. Saielli, *Acc. Chem. Res.*, 2026, **59**, 1256–1266.

24 Y. Nomura, Y. Takeuchi and N. Nakagawa, *Tetrahedron Lett.*, 1969, **10**, 639–642.

View Article Online
DOI: 10.1039/D6CP01530A

25 P. Pyykkö, A. Görling and N. Rösch, *Mol. Phys.*, 1987, **61**, 195–205.

26 M. Kaupp, O. L. Malkina, V. G. Malkin and P. Pyykkö, *Chem. Eur. J.*, 1998, **4**, 118–126.

27 A. M. Kantola, P. Lantto, J. Vaara and J. Jokisaari, *Phys. Chem. Chem. Phys.*, 2010, **12**, 2679–2692.

28 Y. Y. Rusakov, I. L. Rusakova and L. B. Krivdin, *Int. J. Quantum Chem.*, 2016, **116**, 1404–1412.

29 L. Visscher, T. Enevoldsen, T. Saue, H. J. A. Jensen and J. Oddershede, *J. Comput. Chem.*, 1999, **20**, 1262–1273.

30 T. Enevoldsen, L. Visscher, T. Saue, H. J. A. Jensen and J. Oddershede, *J. Chem. Phys.*, 2000, **112**, 3493–3498.

31 S. S. Gomez, R. H. Romero and G. A. Aucar, *J. Chem. Phys.*, 2002, **117**, 7942–7946.

32 P. Lantto, R. H. Romero, S. S. Gómez, G. A. Aucar and J. Vaara, *J. Chem. Phys.*, 2006, **125**, 184113.

33 A. F. Maldonado and G. A. Aucar, *Phys. Chem. Chem. Phys.*, 2009, **11**, 5615–5627.

34 J. I. Melo, A. Maldonado and G. A. Aucar, *Theor. Chem. Acc.*, 2011, **129**, 483–494.

35 A. F. Maldonado, G. A. Aucar and J. I. Melo, *J. Mol. Model.*, 2014, **20**, 2417.

36 J. Autschbach and S. Zheng, *Annu. Reports NMR Spectrosc.*, 2009, **67**, 1–95.

View Article Online
DOI: 10.1039/D6CP01530A

37 J. Vícha, J. Novotný, S. Komorovsky, M. Straka, M. Kaupp and R. Marek, *Chem. Rev.*, 2020, **120**, 7065–7103.

38 Z.-L. Xue and T. M. Cook, eds. J. Reedijk and K. Poeppelmeier, Elsevier, Oxford, 2023, pp. 660–744.

39 Y. A. Buslaev and E. G. Ilyin, *J. Fluor. Chem.*, 1974, **4**, 271–281.

40 M. J. Frisch, G. W. Trucks, H. B. Schlegel, G. E. Scuseria, M. A. Robb, J. R. Cheeseman, G. Scalmani, V. Barone, G. A. Petersson, H. Nakatsuji, X. Li, M. Caricato, A. V. Marenich, J. Bloino, B. G. Janesko, R. Gomperts, B. Mennucci, H. P. Hratchian, J. V. Ortiz, A. F. Izmaylov, J. L. Sonnenberg, D. Williams-Young, F. Ding, F. Lipparini, F. Egidi, J. Goings, B. Peng, A. Petrone, T. Henderson, D. Ranasinghe, V. G. Zakrzewski, J. Gao, N. Rega, G. Zheng, W. Liang, M. Hada, M. Ehara, K. Toyota, R. Fukuda, J. Hasegawa, M. Ishida, T. Nakajima, Y. Honda, O. Kitao, H. Nakai, T. Vreven, K. Throssell, J. A. J. Montgomery, J. E. Peralta, F. Ogliaro, M. J. Bearpark, J. J. Heyd, E. N. Brothers, K. N. Kudin, V. N. Staroverov, T. A. Keith, R. Kobayashi, J. Normand, K. Raghavachari, A. P. Rendell, J. C. Burant, S. S. Iyengar, J. . Tomasi, M. Cossi, J. M. Millam, M. Klene, C. Adamo, R. Cammi, J. W. Ochterski, R. L. Martin, K. Morokuma, O. Farkas, J. B. Foresman and D. J. Fox, 2016.

41 E. J. Baerends, T. Ziegler, A. J. Atkins, J. Autschbach, D. Bashford, O. Baseggio, A. Bérces, F. M. Bickelhaupt, C. Bo, P. M. Boerritger, L. Cavallo, C. Daul, D. P. Chong, D. V Chulhai, L. Deng, R. M. Dickson, J. M. Dieterich, D. E. Ellis, M. van Faassen, A. Ghysels, A. Giammona, S. J. A. van Gisbergen, A. Goez, A. W. Götz, S. Gusarov, F. E. Harris, P. van

View Article Online
DOI: 10.1039/D6CP01530A

den Hoek, Z. Hu, C. R. Jacob, H. Jacobsen, L. Jensen, L. Joubert, J. W. Kaminski, G. van Kessel, C. König, F. Kootstra, A. Kovalenko, M. Krykunov, E. van Lenthe, D. A. McCormack, A. Michalak, M. Mitoraj, S. M. Morton, J. Neugebauer, V. P. Nicu, L. Noodleman, V. P. Osinga, S. Patchkovskii, M. Pavanello, C. A. Peeples, P. H. T. Philipsen, D. Post, C. C. Pye, H. Ramanantoanina, P. Ramos, W. Ravenek, J. I. Rodríguez, P. Ros, R. Rüger, P. R. T. Schipper, D. Schlüns, H. van Schoot, G. Schreckenbach, J. S. Seldenthuis, M. Seth, J. G. Snijders, M. Solà, S. M., M. Swart, D. Swerhone, G. te Velde, V. Tognetti, P. Vernooijs, L. Versluis, L. Visscher, O. Visser, F. Wang, T. A. Wesolowski, E. M. van Wezenbeek, G. Wiesenekker, S. K. Wolff, T. K. Woo and A. L. Yakovlev, 2019.

42 G. te Velde, F. M. Bickelhaupt, E. J. Baerends, C. F. Guerra, S. J. A. van Gisbergen, J. G. Snijders and T. Ziegler, *J. Comput. Chem.*, 2001, **22**, 931–967.

43 E. van Lenthe, E. J. Baerends and J. G. Snijders, *J. Chem. Phys.*, 1994, **101**, 9783–9792.

44 S. K. Wolff, T. Ziegler, E. van Lenthe and E. J. Baerends, *J. Chem. Phys.*, 1999, **110**, 7689–7698.

45 M. Repisky, S. Komorovsky, M. Kadek, L. Konecny, U. Ekström, E. Malkin, M. Kaupp, K. Ruud, O. L. Malkina and V. G. Malkin, *J. Chem. Phys.*, 2020, **152**, 184101.

46 S. Komorovsky, M. Repisky, V. G. Malkin, O. L. Malkina, M. Kaupp and K. Ruud, 2019.

47 J. Tomasi, B. Mennucci and E. Cances, *J. Mol. Struct.*, 1999, **464**, 211–226.

48 J. Tomasi, B. Mennucci and R. Cammi, *Chem. Rev.*, 2005, **105**, 2999–3093.

View Article Online
DOI: 10.1039/D6CP01530A

49 A. Klamt, *Wiley Interdiscip. Rev. Comput. Mol. Sci.*, 2011, 1, 699–709.

50 A. D. Becke, *Phys. Rev. a*, 1988, **38**, 3098–3100.

51 J. P. Perdew, *Phys. Rev. B*, 1986, **34**, 7406.

52 P. J. Stephens, F. J. Devlin, C. F. Chabalowski and M. J. Frisch, *J. Phys. Chem.*, 1994, **98**, 11623–11627.

53 S. Grimme, S. Ehrlich and L. Goerigk, *J. Comput. Chem.*, 2011, **32**, 1456–1465.

54 C. Adamo and V. Barone, *J. Chem. Phys.*, 1999, **110**, 6158–6170.

55 J.-D. Chai and M. Head-Gordon, *Phys. Chem. Chem. Phys.*, 2008, **10**, 6615–6620.

56 F. Weigend and R. Ahlrichs, *Phys. Chem. Chem. Phys.*, 2005, **7**, 3297–3305.

57 D. Andrae, U. Häußermann, M. Dolg, H. Stoll and H. Preuß, *Theor. Chim. Acta*, 1990, **77**, 123–141.

58 B. P. Pritchard, D. Altarawy, B. Didier, T. D. Gibson and T. L. Windus, *J. Chem. Inf. Model.*, 2019, **59**, 4814–4820.

59 D. Feller, *J. Comput. Chem.*, 1996, **17**, 1571–1586.

60 K. L. Schuchardt, B. T. Didier, T. Elsethagen, L. Sun, V. Gurumoorthi, J. Chase, J. Li and T. L. Windus, *J. Chem. Inf. Model.*, 2007, **47**, 1045–1052.

61 C. T. Lee, W. T. Yang and R. G. Parr, *Phys. Rev. B*, 1988, **37**, 785–789.

View Article Online
DOI: 10.1039/D6CP01530A

62 A. D. Becke, *J. Chem. Phys.*, 1993, **98**, 1372–1377.

63 Fluorine Chemical Shift Table, nmr.chem.ucsb.edu/docs/19Fshifts.html.

64 G. Saielli, *J. Comput. Chem.*, 2023, **44**, 2016–2029.

65 B. B. Mascitti, G. Zanoni, F. de Biasi, F. Rastrelli and G. Saielli, *Phys. Chem. Chem. Phys.*, 2025, **27**, 16326–16335.

66 G. Saielli, *Inorganica Chim. Acta*, 2026, **600**, 123261.

67 G. Casella, A. Bagno, S. Komorovsky, M. Repisky and G. Saielli, *Chem. Eur. J.*, 2015, **21**, 18834–18840.

View Article Online
DOI: 10.1039/D6CP01530A

Data availability

The data supporting this article have been included as part of the Supplementary Information